Wireless Location Estimation With the Assistance of Virtual Base Stations

Chien-Hua Chen, *Student Member, IEEE*, Kai-Ten Feng, *Member, IEEE*,
Chao-Lin Chen, and Po-Hsuan Tseng, *Student Member, IEEE*

Abstract—In recent years, wireless location estimation has attracted a significant amount of attention in different areas. Various types of radio signals are applied for the development of location-estimation algorithms. In this paper, the range measurements acquired from the received time-based information are adopted, and the modified least square (LS) method is utilized to process the raw data and to finally locate the target object. Practical issues, such as the nonline-of-sight (NLOS) errors and the geometric dilution of precision (GDOP) effect, are of concern. The NLOS error will cause a large nonnegative bias while measuring the propagation delay, which will lead to an unreliable result for location estimation. On the other hand, a large GDOP value corresponds to a poor geometric topology, which will result in inferior performance by adopting most of the existing location algorithms. The proposed location-estimation algorithms with virtual base stations (VBSs) will both mitigate the influence from the NLOS errors by imposing the geometric constraints and reduce the GDOP effect by incorporating the assisted VBSs. Two iterative schemes are proposed, including the center-of-gravity-based VBS (VBS-CG) and the minimal GDOP-based VBS (VBS-MG) algorithms, to determine the required number and the locations of the assisted VBSs. The proposed VBS algorithms are compared with other existing location-estimation schemes via simulations. The performance of the VBS-MG algorithm is observed to outperform the other schemes, particularly under the environments with larger NLOS errors and poor geometric layouts.

Index Terms—Geometric dilution of precision (GDOP), non-line-of-sight (NLOS) errors, time of arrival (TOA), two-step least square (LS) method, wireless location estimation.

I. Introduction

WIRELESS positioning techniques have widely been studied over the past few decades. The quality of service of the positioning accuracy has been announced after the issuance of the emergency 911 (E-911) subscriber safety service [1]. With the assistance of the information derived from the posi-

C.-H. Chen, K.-T. Feng, and P.-H. Tseng are with the Department of Communications Engineering, National Chiao Tung University, Hsinchu 300, Taiwan (e-mail: chchen.cm93g@nctu.edu.tw; ktfeng@mail.nctu.edu.tw; walker.cm90@nctu.edu.tw).

C.-L. Chen is with TrendChip Technologies Corporation, Hsinchu 310, Taiwan (e-mail: sart.cm92g@nctu.edu.tw).

tioning system, the required performance and objectives for the mobile station (MS) can be achieved with augmented robustness. In recent years, there have been increasing demands for commercial applications to adopt location information within their system design, such as navigation systems, location-based billing, health care systems, and wireless sensor networks. With emerging interests in location-based services, location-estimation algorithms with enhanced precision have become necessary for applications under different circumstances.

A variety of wireless location techniques have been studied and investigated [2]–[4]. The network-based location-estimation schemes have widely been proposed and employed in wireless communication systems. These schemes locate the position of the MS based on the measured radio signals from its neighborhood base stations (BSs). The representative algorithms for the network-based location-estimation techniques are the time of arrival (TOA) and the time difference of arrival (TDOA). The TOA scheme estimates the MS's location by measuring the arrival time of the radio signals coming from different wireless BSs, whereas the TDOA method measures the time difference between the arriving radio signals. It is recognized that the equations associated with the network-based location-estimation schemes are inherently nonlinear. The uncertainties induced by the measurement noises make it more difficult to acquire the estimated MS's position with tolerable precision. The Taylor series expansion (TSE) [5], the two-step least square (LS) algorithm [6], and the linear line of position (LLOP) scheme [7] have been studied to provide reasonable accuracy for location estimation. However, these techniques are primarily designed for location estimation under line-of-sight (LOS) environments. Non-LOS (NLOS) situations, which mostly occur in urban or suburban areas, greatly affect the precision in most location-estimation schemes.

The measurements of the propagation time significantly dominate the performance of these time-based location algorithms. The NLOS error, which is the additional propagation time (i.e., with a positive value), has been observed as a dominating issue for time-based location estimation [8]. The fact that NLOS error can be extended to around 600 m within the IS-95 code-division multiple-access networks has been investigated [9]. The large bias in the range measurement will severely diminish the accuracy of network-based location-estimation algorithms. The range scaling algorithm (RSA) proposed in [10] alleviates NLOS errors by considering the geometric layout between the MS and its associated BSs. However, the RSA approach requires solving an optimization problem based on

a nonlinear objective function. The inefficiency incurred by the RSA algorithm may not be feasible for application in practical systems.

In this paper, the location-estimation technique along with the assistance of virtual base stations (VBSs) is proposed to obtain location estimation of the MS. The concept of the VBS algorithm is to transform the geometric relationship between the MS and its neighborhood BSs into a set of VBSs by considering the geometric dilution of precision (GDOP) [11] effects. The proposed VBS schemes integrate the geometric information into the conventional two-step LS algorithm for obtaining the position of the MS. The location-estimation problem is reformulated based on the geometric layout extended by the VBSs. Two types of VBS algorithms, i.e., the center-of-gravity-based (VBS-CG) scheme and the minimum GDOP-based (VBS-MG) scheme, are proposed as the precision-enhanced schemes for location estimation. Reasonable location estimation can be acquired within three computing iterations, particularly under the poor GDOP and NLOS environments. The numerical results obtained through simulations show that the proposed VBS approach can achieve higher estimation accuracy for the MS's location compared with other existing methods.

The remainder of this paper is organized as follows: Section II describes the related work for wireless location-estimation techniques. The modeling of the signal measurements, the GDOP metrics, and the two-step LS method are briefly reviewed in Section III. The proposed VBS algorithms are explained in Section IV. The performance evaluation of the proposed schemes is conducted in Section V via simulations. Section VI draws conclusions.

II. RELATED WORK

Different location-estimation schemes have been proposed to acquire the MS's position. Various types of information [e.g., the signal traveling distance, the received angle of the signal, and the receiving signal strength (RSS)] are involved to facilitate the algorithm design for location estimation. The primary objective in most of the location-estimation algorithms is to obtain higher estimation accuracy with promoted computational efficiency. Superresolution schemes are proposed as in [12]–[15]. The eigendecomposition method is involved to extract the location parameters from the covariance matrix of the received signals. Although the superresolution methods can be utilized to classify the various types of parameters, these schemes are observed to suffer from computational complexity and high sensitivity to large noises.

A beamforming system [16]–[18] is a space–time processor that operates at the output of a sensor array. It provides spatial filtering capability with an enhanced signal-to-noise ratio, which results in reduction of the estimation errors. However, the complexity of the beamforming system makes the associated location-estimation techniques difficult to practically realize. Instead of exploiting the spatial and temporal information of the signal, the location fingerprinting techniques locate the MS based on the RSS [19]–[21]. These techniques involve two phases for location estimation as follows: 1) the offline phase

to build up a signal signature database for a specific service area and 2) the online phase to compare the measured RSS with the database. It has been noticed that both the extended training of the RSS and a considerable size of database are required for the location fingerprinting schemes. Ray optical approaches [22]–[25] for location estimation aggregate the received signals, which are reflected or diffracted by various obstacles after launching from a transmitter. However, tremendous computation of the field strength is unavoidable at the receiver as the number of reflective or diffractive signals is increased.

There are also different approaches exploiting linearized methods to achieve computational efficiency while obtaining approximate estimation of the MS's position. The TSE method was utilized in [5] to acquire the location estimation of the MS from the TOA measurements. The method requires iterative processes to obtain the location estimate from a linearized system. The major drawback of the TSE scheme is that it may suffer from the convergence problem due to an incorrect initial guess of the MS's position. The two-step LS method was adopted to solve the location-estimation problem from different types of measurement inputs [6], [26], [27]. It is an approximate realization of the maximum-likelihood estimator and does not require iterative processes. The two-step LS scheme is advantageous in its computational efficiency with adequate accuracy for location estimation. However, the scheme is demonstrated to be feasible only to acquire the estimated position of the MS under the LOS circumstances. Instead of utilizing circular line of position methods (e.g., the TSE and the two-step LS schemes), the LLOP approaches [7], [28] are presented as a new interpretation for the cell geometry from the TOA measurements. By transforming the circular intersections into the corresponding independent lines, the LS method can therefore be applied to estimate the position of the MS.

While most of the location-estimation schemes as aforementioned did not explicitly consider the effect from the NLOS error, there are also other researchers who have proposed [10], [29]–[35] to either identify or mitigate the NLOS error. The residual weighting algorithm (Rwgh) proposed in [29] exploits the LS estimator and imposes weighting coefficients to each of the intermediate estimates for the identification of the NLOS error. The primary problem within the Rwgh algorithm is the considerable computation time associated with the enlarged permutation. By accumulating the time history of the range measurements, decision hypotheses can be utilized and constructed to distinguish the NLOS error from its LOS signal. The NLOS-contaminated signal can be corrected by calculating the stochastic characteristics (e.g., the means and the standard deviations) of the signals [30], [31], whereas the Kalman filtering technique is adopted in [32] for NLOS identification. The corrected signal can be proceeded with other positioning schemes, and therefore, better estimation can be expected. However, an additional amount of computation time is required for these schemes to obtain feasible decisions on the hypothesis tests. On the other hand, the NLOS error can be reduced in the RSA [10] and the geometric-assisted location-estimation [33], [34] schemes without knowing the prior information of the range

measurements. However, the iterative optimization processes for acquiring the scaling factor can be the bottleneck of the RSA algorithm.

It can be observed from the previous work that most location-estimation schemes are primarily suitable for the LOS environment, whereas others involve complicated computation to deal with the NLOS errors. The proposed VBS algorithms, as will be described in the remaining sections, can provide better location estimation by considering both the NLOS errors and the geometric relationship between the MS and its associated BSs.

III. PRELIMINARIES

In this section, mathematical modeling of the signal measurements is formulated in Section III-A. Section III-B briefly summarizes the concept of the GDOP metrics. The conventional two-step LS method for location estimation is reviewed in Section III-C.

A. Modeling of the Signal Measurements

To facilitate the design of the proposed VBS algorithms, the signal model for the TOA measurements is presented in this section. The TOA measurement t_ℓ from the ℓth BS is obtained by

$$t_\ell = \frac{r_\ell}{c} = \frac{1}{c}(\zeta_\ell + n_\ell) = \frac{1}{c}(\zeta_\ell + n_{\ell,m} + n_{\ell,nl}) \quad (1)$$

where $\ell = 1, 2, \ldots, N_b$. The parameter c represents the speed of light, N_b is the total number of available BSs, and r_ℓ denotes the measured relative distance between the MS and the ℓth BS. r_ℓ is contaminated with noises n_ℓ from the TOA measurement, which includes the measurement noise $n_{\ell,m}$ and the NLOS error $n_{\ell,nl}$. It is noted that the NLOS error $n_{\ell,nl}$ is a positive value due to the longer distance traversed by the NLOS effect. The noiseless relative distance ζ_ℓ between the MS and the ℓth BS is represented as

$$\zeta_\ell = \|\boldsymbol{x} - \boldsymbol{x}_\ell\| \quad (2)$$

where $\boldsymbol{x} = (x, y)$ indicates the MS's position, and $\boldsymbol{x}_\ell = (x_\ell, y_\ell)$ is the location of the ℓth BS.

B. GDOP Metrics

GDOP [11] is defined as the ratio between the location-estimation error and the associated measurement error. It is utilized as an index for observing the location precision of the MS under different geometric locations within the network, e.g., the cellular or the satellite network. Consider the MS's location under the 2-D coordinates, the GDOP value obtained at $\boldsymbol{x}$ can be represented as

$$G_{\boldsymbol{x}} = \left[\text{trace}(\mathbf{M}^T\mathbf{M})^{-1}\right]^{\frac{1}{2}} \quad (3)$$

where

$$\mathbf{M} = \begin{bmatrix} \frac{x-x_1}{\zeta_1} & \frac{y-y_1}{\zeta_1} \\ \cdot & \cdot \\ \frac{x-x_\ell}{\zeta_\ell} & \frac{y-y_\ell}{\zeta_\ell} \\ \cdot & \cdot \\ \frac{x-x_{N_b}}{\zeta_{N_b}} & \frac{y-y_{N_b}}{\zeta_{N_b}} \end{bmatrix}. \quad (4)$$

It is noted that the elements in $\mathbf{M}$ can be acquired from (2). A small GDOP value corresponds to an effective positioning geometry that allows for a relatively inaccurate measurement. It has been shown in [11] that the minimum GDOP value frequently occurs around the center of the network layout, e.g., the minimum GDOP inside a K-side $(K \geq 3)$ regular polygon is shown to take place at the center of the layout, and the value is obtained as $G_x = 2/\sqrt{K}$. Moreover, the GDOP value and the Cramér–Rao lower bound are demonstrated to be identical, given a Gaussian-distributed noise model [36].

C. Two-Step LS Method

The two-step LS scheme is utilized as the baseline formulation for the proposed VBS algorithms. The concept of the two-step LS method is to acquire an intermediate location estimate in the first step with the definition of a new variable β, which is mathematically related to the MS's position (i.e., $\beta = x^2 + y^2$). At this stage, the variable β is assumed to be uncorrelated to the MS's position. This assumption effectively transforms the nonlinear equations for location estimation into a set of linear equations, which can directly be solved by the LS method. It is also noted that the selection of β provides a feasible first-step location estimation compared with the random initial guess in the iterative linear LS method, e.g., the TSE scheme. Moreover, the elements within the associated covariance matrix are selected based on the standard deviation from the measurements. The variations within the corresponding signal paths are therefore considered within the problem formulation.

The second step of the method primarily considers the relationship that the variable β is equal to $x^2 + y^2$, which was originally assumed to be uncorrelated in the first step. An improved location estimation can be obtained after the adjustment from the second step. The detailed algorithm for the two-step LS method for location estimation can be found in [6], [26], and [27].

IV. PROPOSED LOCATION-ESTIMATION ALGORITHMS WITH THE ASSISTANCE OF VBSS

In this section, the proposed VBS algorithms are described in detail. The observation from the GDOP effect is addressed in Section IV-A. Section IV-B describes the concepts and motivations of the proposed VBS schemes, whereas the formulation of the algorithm is presented in Section IV-C. The VBS selection schemes, i.e., the VBS-CG and VBS-MG methods, are presented in Section IV-D.
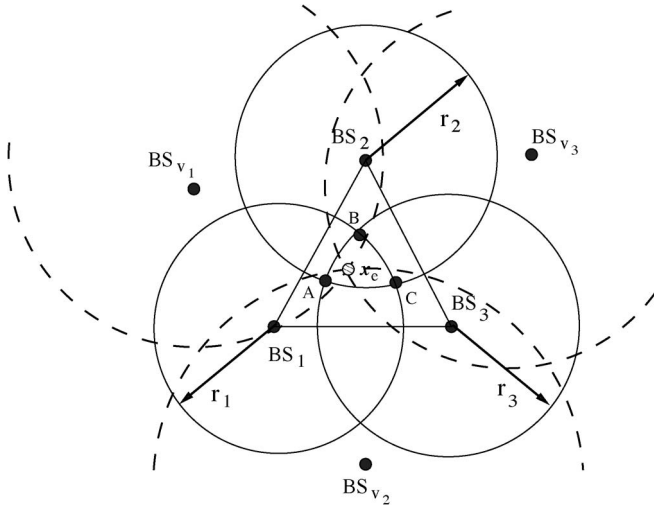
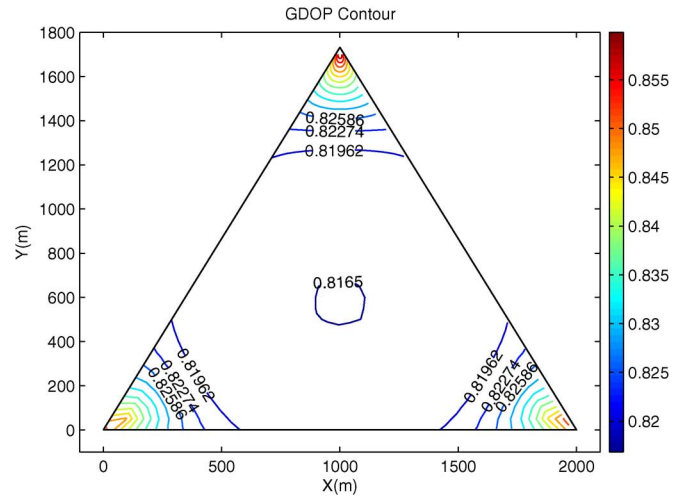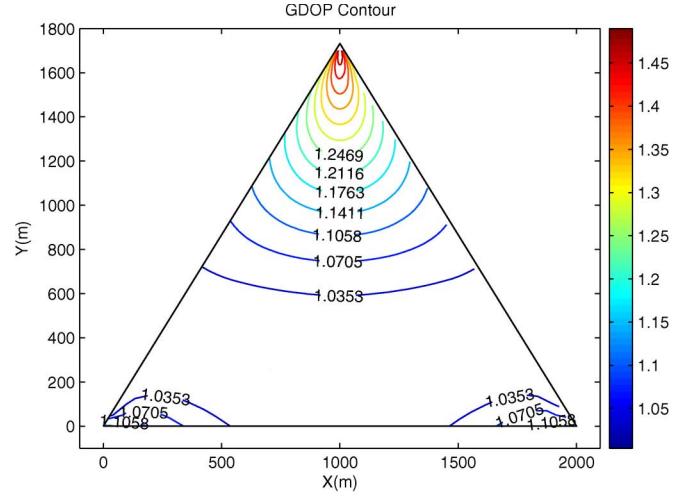Fig. 1.   Schematic diagram of the TOA-based location estimation with VBSs.

Fig. 2.   (Upper plot) GDOP contours using three TOA measurements. (Lower plot) GDOP contours with one VBS at the center of the triangular area.
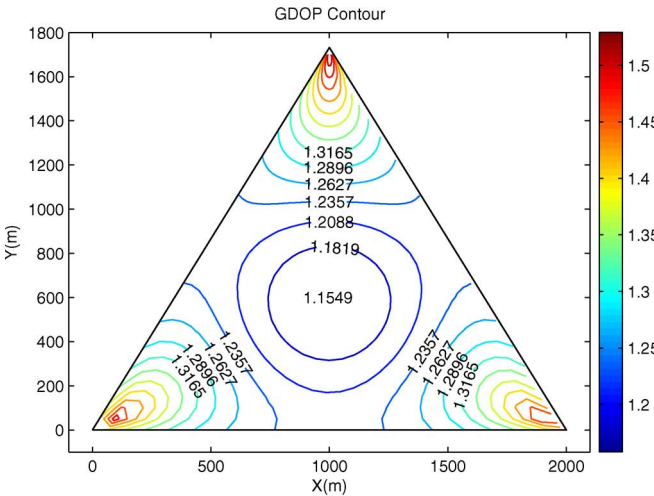

Fig. 3.   (Upper plot) GDOP contours with one VBS outside the triangular area. (Lower plot) GDOP contours with three VBSs outside the triangular area.

A. Observation From the GDOP Effect

As mentioned in Section III-B, the GDOP value is employed as a metric to determine the geometric effect on the precision of location estimation for the MS. To investigate the GDOP effect,

a cell layout with three TOA measurements is considered, as shown in Fig. 1. The three BSs are assumed to be located at coordinates $(0, 0)$, $(1000, 1000\sqrt{3})$, and $(2000, 0)$, in meters. The locations of the MS are designed to be within the enclosed triangular area formed by the three BSs. i.e., points BS_1, BS_2, and BS_3. The upper plot of Fig. 2 shows the GDOP effect for the three TOA measurements within the triangular region. It can be seen that there is a worse GDOP effect (i.e., with higher GDOP values) around the areas close to the three BSs, as compared with the other regions within the triangular area. To further observe the GDOP effect, it is possible to provide an additional BS with an adjustable location within the network. The lower plot of Fig. 2 illustrates the GDOP effect with the fourth BS located at the center of the triangle $BS_1BS_2BS_3$, whereas the upper plot of Fig. 3 shows the same thing with the fourth BS situated outside the triangular area, i.e., at point BS_{v2}, as shown in Fig. 1. It can be observed from the lower plot of Fig. 2 that the GDOP values are decreased by placing the fourth BS within the triangular region. On the other hand, it is interesting to find that the high GDOP value around BS_1 and BS_3 can be reduced by the fourth BS situated outside the triangular area (as shown in the upper plot of Fig. 3). Moreover, it can be seen from the lower plot of Fig. 3 that the GDOP values around the three

BSs can be decreased by adding another three BSs (i.e., BS_{v1}, BS_{v2}, and BS_{v3}, as shown in Fig. 1) around the corresponding locations outside the triangular region. It is also noted that the overall GDOP values are decreased.

From the aforementioned observation, it is found to be beneficial to provide additional BSs (with feasible adjustment of their locations) to improve the poor GDOP effect within the network. However, in reality, it is not practical to arbitrarily install additional BSs. As will be explained in the next section, the mathematically formulated VBSs are applied in the proposed VBS schemes. The positions of the VBSs determine the associated parameters within their corresponding geometric constraints. Without physically installing additional BSs, the proposed schemes can mitigate the poor GDOP effect with the assistance of VBSs. The following sections will illustrate the overview and formulation of the proposed VBS algorithms.

B. Overview of the VBS Algorithms

Fig. 4 illustrates the schematic diagram of the proposed VBS formulation, including the iterative processes for both the VBS location-estimation and the VBS selection schemes. It is noted that two VBS selection schemes (i.e., the VBS-CG and VBS-MG) are adopted to determine the locations of the VBSs. At the initial stage, the MS's position is estimated (i.e., $\hat{\boldsymbol{x}}^{(0)}$) using the VBS location-estimation scheme with only the measurement inputs from the physical BSs, i.e., using the conventional two-step LS method based on $\boldsymbol{x}_\ell$ and r_ℓ. The concept of the proposed VBS algorithm is to design a mathematically formulated VBS, i.e., $\boldsymbol{x}_{v,1}$, such that the previously estimated MS will be situated in a better *virtual* layout. In the VBS-CG selection scheme, the VBS is assigned such that $\hat{\boldsymbol{x}}^{(0)}$ is located at the center of gravity of the extended virtual layout, whereas $\hat{\boldsymbol{x}}^{(0)}$ will possess the minimal GDOP value by adopting the VBS-MG selection scheme. After obtaining the location of the VBS $\boldsymbol{x}_{v,1}$, a new location estimate $\hat{\boldsymbol{x}}^{(1)}$ can be acquired by including $\boldsymbol{x}_{v,1}$ (associated with the original measurement inputs $\boldsymbol{x}_\ell$) within the formulation of the VBS location estimation. The iteration will be terminated until the difference between two consecutive location estimates is less than a prespecified threshold, as shown in Fig. 4. Therefore, the final estimated MS's position can be obtained by iteratively selecting and adding VBSs based on either the VBS-MG or VBS-CG schemes.

As illustrated in Fig. 1, a 2-D TOA-based location estimation is considered. The measured distances between the BSs and the MS are denoted as r_ℓ for $\ell = 1$, 2, and 3. It is noted that the three circles that define the TOA measurements will intersect to a single point (i.e., the MS's position) if the measurements are LOS and are free of the measurement noises. The overlap region confined within the points A, B, and C (as shown in Fig. 1) is primarily incurred by the NLOS errors. It was observed that the location estimation by using the conventional two-step LS method may fall around the boundaries of the three arcs AB, BC, and CA, i.e., either inside or outside these arcs. Since the overlap region (i.e., constrained by the points A, B, and C) grows as the NLOS errors are increased, the location
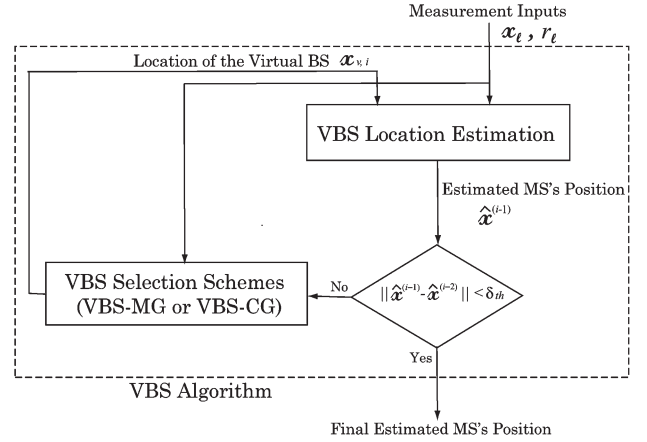

Fig. 4. Iterative process of the proposed VBS algorithms.

estimation of the MS acquired by the two-step LS method will result in deficient accuracy. In other words, the location estimate will fall around the boundaries of the enlarged arcs AB, BC, and CA.

It has been proven in [33] that the location of the MS should always fall inside the overlap region under the environment with large NLOS errors, i.e., while the NLOS error is comparably larger than the absolute value of the measurement noise. Based on the aforementioned observation, the primary objective of the proposed VBS algorithms is to confine the location estimate within the overlap region by including the geometric constraints into the two-step LS method. The locations of the VBSs can be arbitrarily placed within the network, which determine the parameters in their associated geometric constraints. The following section will illustrate the formulation of the VBS algorithms, which corresponds to the inclusion of m VBSs within the two-step LS method.

C. Formulation of the VBS Location-Estimation Algorithms

As illustrated in Fig. 1, three BSs associated with the three TOA measurements are utilized for the location estimation of the MS. The overlap region (i.e., confined by the arcs AB, BC, and CA) is formed with the assumption that there is at least one NLOS error that occurred from one of the three TOA range measurements. Since the objective of the proposed VBS algorithms is to confine the estimated MS's position within the region of ABC, the following definitions and a constrained cost function are defined.

Definition 1 (Virtual Distance): The parameter γ_i (for $i = 1, \ldots, m$) is defined as the ith virtual distance between the MS's position and the three intersecting points A, B, and C, i.e.,

$$\gamma_i = \left[\sum_\mu \alpha_{\mu,i} \| \boldsymbol{x} - \boldsymbol{x}_\mu \|^2 \right]^{\frac{1}{2}} \tag{5}$$

where $\boldsymbol{x}$ is the MS's location; $\boldsymbol{x}_\mu$ represents the intersecting points around the overlap region, i.e., $\boldsymbol{x}_\mu = \boldsymbol{x}_a$, $\boldsymbol{x}_b$, and $\boldsymbol{x}_c$ in this case, where $\boldsymbol{x}_a = (x_a, y_a)$, $\boldsymbol{x}_b = (x_b, y_b)$, and $\boldsymbol{x}_c = (x_c, y_c)$ are the corresponding coordinates of the points A, B, and C. $\alpha_{\mu,i}$'s (for $\mu = a$, b, and c) are the BS parameters that

are determined by the location of the VBS, which will be described later.

It is noted that the value of γ_i varies as the three coordinates $\boldsymbol{x}_a$, $\boldsymbol{x}_b$, and $\boldsymbol{x}_c$ are changed. On the other hand, an expected MS's position $\boldsymbol{x}_e$ is chosen to be located within the triangular area ABC to fulfill the constraints from the geometric layout. The corresponding ith *expected virtual distance* $\gamma_{e,i}$ can be defined in the following.

Definition 2 (Expected Virtual Distance): The ith expected virtual distance $\gamma_{e,i}$ is defined as

$$\gamma_{e,i} = \left[\sum_\mu \alpha_{\mu,i} \|\boldsymbol{x}_e - \boldsymbol{x}_\mu\|^2\right]^{\frac{1}{2}} = \gamma_i + n_{\gamma,i} \quad (6)$$

where $\boldsymbol{x}_e$ is the expected position of the MS, and $n_{\gamma,i}$ denotes the error induced by the computed deviation between $\gamma_{e,i}$ and γ_i.

The major objective of adapting the geometric constraint in the VBS algorithms is to minimize the cost function $f = \|\gamma_i - \gamma_{e,i}\|$ with the constraints as in (6), i.e., to minimize the deviation between the ith *virtual distance* γ_i and the *expected virtual distance* $\gamma_{e,i}$. The selection of the expected MS's position $\boldsymbol{x}_e$ is obtained by considering the signal variations from the three TOA measurements. The coordinates of $\boldsymbol{x}_e = (x_e, y_e)$ are chosen with different weights (w_1, w_2, w_3) w.r.t. the A, B, and C points of the triangle, i.e.,

$$\boldsymbol{x}_e = \sum_{k=1}^n w_k I_k \quad (7)$$

where $n = 3$ in this case. I_k denotes the intersecting points from the TOA measurements, i.e., $I_1 = \boldsymbol{x}_a$, $I_2 = \boldsymbol{x}_b$, and $I_3 = \boldsymbol{x}_c$. The weighting coefficients w_k are defined based on the effects from both the standard deviations and the relative distance w.r.t. the corresponding TOA measurements, which can be obtained as in [33].

Based on an appropriate selection of the weighting coefficients, the expected MS's position $\boldsymbol{x}_e$ is obtained. The ith *expected virtual distance* $\gamma_{e,i}$ can therefore be computed from (6). The proposed VBS algorithms can be formulated by solving the two-step LS problem with the additional geometric constraints, which are determined by the locations of the VBSs. The solution is obtained by minimizing both the errors coming from the three TOA measurements [as in (1)] and the deviations between the *expected virtual distances* and the *virtual distances* [as in (6)]. By rearranging and combining (1) and (6) in the matrix format, the following equation can be obtained:

$$\mathbf{H}\boldsymbol{z} = \mathbf{J} + \psi \quad (8)$$

where $\boldsymbol{z} = [\,x \quad y \quad \beta\,]^T$, and

$$\mathbf{H} = \begin{bmatrix} \mathbf{H}_{\text{TOA}}^{3\times3} \\ \mathbf{H}_\gamma^{m\times3} \end{bmatrix} = \begin{bmatrix} -2x_1 & -2y_1 & 1 \\ -2x_2 & -2y_2 & 1 \\ -2x_3 & -2y_3 & 1 \\ -2x_{v,1} & -2y_{v,1} & 1 \\ . & . & . \\ -2x_{v,m} & -2y_{v,m} & 1 \end{bmatrix} \quad (9)$$

$$\mathbf{J} = \begin{bmatrix} \mathbf{J}_{\text{TOA}}^{3\times1} \\ \mathbf{J}_\gamma^{m\times1} \end{bmatrix} = \begin{bmatrix} r_1^2 - \kappa_1 \\ r_2^2 - \kappa_2 \\ r_3^2 - \kappa_3 \\ \gamma_{e,1}^2 - \kappa_{\gamma,1} \\ . \\ \gamma_{e,m}^2 - \kappa_{\gamma,m} \end{bmatrix}. \quad (10)$$

The corresponding coefficients are given by

$$\beta = x^2 + y^2 \quad (11)$$

$$\kappa_\ell = x_\ell^2 + y_\ell^2, \qquad \ell = 1, 2, 3 \quad (12)$$

$$x_{v,i} = \alpha_{a,i} x_a + \alpha_{b,i} x_b + \alpha_{c,i} x_c \quad (13)$$

$$y_{v,i} = \alpha_{a,i} y_a + \alpha_{b,i} y_b + \alpha_{c,i} y_c \quad (14)$$

$$\kappa_{\gamma,i} = \alpha_{a,i}\left(x_a^2 + y_a^2\right) + \alpha_{b,i}\left(x_b^2 + y_b^2\right)$$
$$+ \alpha_{c,i}\left(x_c^2 + y_c^2\right). \quad (15)$$

The *expected virtual distances* $\gamma_{e,i}$ [as shown in (10)] serve as the virtual measurements, as compared with those true measurements r_ℓ for $\ell = 1$, 2, and 3. It is noticed that $\boldsymbol{x}_{v,i} = (x_{v,i}, y_{v,i})$ represents the coordinate of the ith VBS. The selection schemes for the VBSs will be described in Section IV-C. Since the coordinates of $\boldsymbol{x}_a$, $\boldsymbol{x}_b$, and $\boldsymbol{x}_c$ are obtainable after the three TOA measurements are acquired, the $\alpha_{\mu,i}$'s within the constraint equation (6) can be computed from (13) and (14), associated with $\sum_{\mu=a,b,c} \alpha_{\mu,i} = 1$. It is also noted that (15) is utilized to facilitate the formulation of the matrix $\mathbf{J}$ in (10). Moreover, the noise matrix ψ in (8) can be obtained as

$$\psi = 2c\mathbf{B}\boldsymbol{n} + c^2 \boldsymbol{n}^2 \quad (16)$$

where

$$\mathbf{B} = \text{diag}\{\zeta_1, \zeta_2, \zeta_3, \gamma_1, \dots, \gamma_m\}$$

$$\boldsymbol{n} = [\,n_1 \quad n_2 \quad n_3 \quad n_{\gamma,1}/c \quad \cdots \quad n_{\gamma,m}/c\,]^T.$$

Based on the VBS location-estimation scheme, an intermediate estimate $\hat{\boldsymbol{z}}$ after the first step can be obtained as

$$\hat{\boldsymbol{z}} = [\,\hat{x}_i \quad \hat{y}_i \quad \hat{\beta}\,]^T = (\mathbf{H}^T \boldsymbol{\Psi}^{-1} \mathbf{H})^{-1} \mathbf{H}^T \boldsymbol{\Psi}^{-1} \mathbf{J} \quad (17)$$

where $(\hat{x}_i, \hat{y}_i)$ is denoted as the intermediate location estimation of the MS after the first step of the algorithm. The weighting matrix $\boldsymbol{\Psi}$ is obtained as

$$\boldsymbol{\Psi} = \boldsymbol{E}[\psi\psi^T] = 4c^2 \mathbf{B}\mathbf{Q}\mathbf{B}. \quad (18)$$

It is noted that $\boldsymbol{\Psi}$ is acquired by neglecting the second term of (16). The matrix $\mathbf{Q}$ becomes

$$\mathbf{Q} = \text{diag}\left\{\sigma_{r_1}^2, \sigma_{r_2}^2, \sigma_{r_3}^2, \sigma_{\gamma_{e,1}}^2 / c^2, \dots, \sigma_{\gamma_{e,m}}^2 / c^2\right\}.$$

It can be observed that $\mathbf{Q}$ represents the covariance matrix for both the TOA measurements and the *expected virtual distances*, where $\sigma_{\gamma_{e,i}}$ corresponds to the standard deviation of $\gamma_{e,i}$. Therefore, the final location estimation after the second step of the VBS location-estimation scheme can be obtained as [26]

$$\hat{\boldsymbol{x}} = [\,\hat{x} \quad \hat{y}\,]^T = \left[(\mathbf{H}'^T \boldsymbol{\Psi}'^{-1} \mathbf{H}')^{-1} \mathbf{H}'^T \boldsymbol{\Psi}'^{-1} \mathbf{J}'\right]^{1/2} \quad (19)$$

where

$$\mathbf{H}' = \begin{bmatrix} 1 & 0 & 1 \\ 0 & 1 & 1 \end{bmatrix}^T$$

$$\mathbf{J}' = [\,\hat{x}_i^2 \quad \hat{y}_i^2 \quad \hat{\beta}\,]^T$$

$$\boldsymbol{\Psi}' = \boldsymbol{E}[\psi'\psi'^T]$$

$$= 4\mathbf{B}'\mathrm{cov}(\hat{\boldsymbol{z}})\mathbf{B}'$$

$$= 4\mathbf{B}'(\mathbf{H}^T\boldsymbol{\Psi}^{-1}\mathbf{H})^{-1}\mathbf{B}'$$

$$\mathbf{B}' = \mathrm{diag}\{\hat{x}_i, \hat{y}_i, 1/2\}.$$

D. Selection Schemes for the VBSs

As mentioned in the previous sections, there are two parameters that need to be acquired within the VBS formulation: the number of VBSs and the locations of these VBSs. Iterative selection schemes will be utilized to determine the feasible number of VBSs to be included within the formulation, whereas the locations of the adopted VBSs will be obtained based on the GDOP metrics. Two VBS selection schemes are proposed, as shown in Fig. 4, i.e., the VBS-CG and VBS-MG methods. The VBS-CG algorithm is a simplified selection scheme that is suitable for topologies with a regular polygon shape, whereas the VBS-MG method will be satisfactory for the generic cases.

1) VBS-CG: As was discussed in Section III-B, it is shown that the GDOP value is minimum at the center of gravity (CG) of a regular polygon [11]. Therefore, the concept of the VBS-CG scheme is to assign the position of the VBS such that the newly estimated MS will be located at a point with a minimum GDOP value, i.e., at the CG of a polygon. For instance, the location estimation of the MS under three TOA measurements is considered, where the three BSs are located at $\boldsymbol{x}_1$, $\boldsymbol{x}_2$, and $\boldsymbol{x}_3$. The MS is initially estimated as $\hat{\boldsymbol{x}}^{(0)}$ without the inclusion of the VBS by using the conventional two-step LS method. The first VBS $\boldsymbol{x}_{v,1}$ can be calculated by placing $\hat{\boldsymbol{x}}^{(0)}$ as the CG of the newly formed four-sided polygon confined by $\mathbf{P}_4(\boldsymbol{x}_1, \boldsymbol{x}_2, \boldsymbol{x}_3, \boldsymbol{x}_{v,1})$, i.e., $\boldsymbol{x}_{v,1} = 4\hat{\boldsymbol{x}}^{(0)} - (\boldsymbol{x}_1 + \boldsymbol{x}_2 + \boldsymbol{x}_3)$. A new estimation for the MS (i.e., $\hat{\boldsymbol{x}}^{(1)}$) can be acquired using the VBS location-estimation scheme (as described in Section IV-C) under the geometric layout of $\mathbf{P}_4(\boldsymbol{x}_1, \boldsymbol{x}_2, \boldsymbol{x}_3, \boldsymbol{x}_{v,1})$. The iteration process (as shown in Fig. 4) continues until the estimation errors are converged, i.e., $\|\hat{\boldsymbol{x}}^{(i)} - \hat{\boldsymbol{x}}^{(i-1)}\| < \delta_{\mathrm{th}}$, where δ_{th} is defined as a prespecified threshold. The following two lemmas identify the locations of the VBSs and the condition for iteration convergence when using the VBS-CG scheme.

Lemma 1: An N_b-shaped polygon of $\mathbf{P}_{N_b}(\boldsymbol{x}_1, \ldots, \boldsymbol{x}_{N_b})$ is assumed as the cell layout for location estimation of the MS. By adapting the VBS-CG algorithm, the location of the VBS ($\boldsymbol{x}_{v,i}$) acquired at the ith iteration can be obtained as

$$\boldsymbol{x}_{v,i} = \begin{cases} (N_b + i)\hat{\boldsymbol{x}}^{(i-1)} - (N_b + i - 1)\hat{\boldsymbol{x}}^{(i-2)}, & i \geq 2 \\ (N_b + 1)\hat{\boldsymbol{x}}^{(0)} - \sum_{j=1}^{N_b} \boldsymbol{x}_j, & i = 1 \end{cases} \quad (20)$$

where i also indicates the total number of VBSs added during i iterations; $\hat{\boldsymbol{x}}^{(i-1)}$ and $\hat{\boldsymbol{x}}^{(i-2)}$ are denoted as the estimated MS's

position acquired at the $(i-1)$th and $(i-2)$th iterations within the VBS-CG scheme, respectively. $\hat{\boldsymbol{x}}^{(0)}$ is the initial estimation of the MS's position obtained via the original two-step LS method.

Proof: Based on the design concept of the VBS-CG algorithm, the location of the first VBS $\boldsymbol{x}_{v,1}$ is obtained by placing the initial MS's estimation $\hat{\boldsymbol{x}}^{(0)}$ as the CG of the extended geometry, i.e., the $(N_b + 1)$-shaped regular polygon of $\mathbf{P}_{N_b}(\boldsymbol{x}_1, \ldots, \boldsymbol{x}_{N_b}, \boldsymbol{x}_{v,1})$. Thus

$$\boldsymbol{x}_{v,1} = (N_b + 1)\hat{\boldsymbol{x}}^{(0)} - \sum_{j=1}^{N_b} \boldsymbol{x}_j \quad (21)$$

which shows the case for $i = 1$ in (20). For $i > 1$, the location of the VBS acquired at the ith iteration can be represented as

$$\boldsymbol{x}_{v,i} = (N_b + i)\hat{\boldsymbol{x}}^{(i-1)} - \sum_{j=1}^{N_b} \boldsymbol{x}_j - \sum_{k=1}^{i-1} \boldsymbol{x}_{v,k} \quad (22)$$

where $\hat{\boldsymbol{x}}^{(i-1)}$ is considered as the CG of the $(N_b + i)$-sided polygon $\mathbf{P}_{(N_b+i)}(\boldsymbol{x}_1, \ldots, \boldsymbol{x}_{N_b}, \boldsymbol{x}_{v,1}, \ldots, \boldsymbol{x}_{v,i})$. Similarly, the location of the VBS obtained at the $(i-1)$th step becomes

$$\boldsymbol{x}_{v,i-1} = (N_b + i - 1)\hat{\boldsymbol{x}}^{(i-2)} - \sum_{j=1}^{N_b} \boldsymbol{x}_j - \sum_{k=1}^{i-2} \boldsymbol{x}_{v,k} \quad (23)$$

where $\hat{\boldsymbol{x}}^{(i-2)}$ is the CG of the $(N_b + i - 1)$-sided polygon $\mathbf{P}_{(N_b+i-1)}(\boldsymbol{x}_1, \ldots, \boldsymbol{x}_{N_b}, \boldsymbol{x}_{v,1}, \ldots, \boldsymbol{x}_{v,i-1})$. By subtracting (23) from (22), the position of the VBS ($\boldsymbol{x}_{v,i}$) at the ith iteration can therefore be obtained for the case of $i \geq 2$ in (20). This completes the proof. ∎

Lemma 2: According to the VBS-CG algorithm, the location of the VBS selected at the ith iteration is obtained as in (20). For all infinite small numbers δ such that $\|\hat{\boldsymbol{x}}^{(i)} - \hat{\boldsymbol{x}}^{(i-1)}\| < \delta$ with $i \geq 2$, the location of the ith VBS ($\boldsymbol{x}_{v,i}$) will converge to the estimated MS's position ($\hat{\boldsymbol{x}}^{(i-1)}$).

Proof: From (20), the location of the VBS acquired at the ith iteration (for $i \geq 2$) can be rewritten as $\boldsymbol{x}_{v,i} = \hat{\boldsymbol{x}}^{(i-1)} + (N_b + i - 1)(\hat{\boldsymbol{x}}^{(i-1)} - \hat{\boldsymbol{x}}^{(i-2)})$. Under the condition that $\|\hat{\boldsymbol{x}}^{(i)} - \hat{\boldsymbol{x}}^{(i-1)}\| < \delta$ for all infinite small δ, the absolute value between the ith VBS and its newly estimated MS's position becomes $\|\boldsymbol{x}_{v,i} - \hat{\boldsymbol{x}}^{(i-1)}\| = \|(N_b + i - 1)(\hat{\boldsymbol{x}}^{(i-1)} - \hat{\boldsymbol{x}}^{(i-2)})\| < (N_b + i - 1) \cdot \delta \approx \delta$. The result shows that the location of the ith VBS will be converged to the estimated MS's position with the existence of an infinite small number δ. This completes the proof. ∎

It is interesting to observe from Lemma 2 that the position of the selected VBS will approach the location of the estimated MS as the VBS selection scheme is converged. This result will further be validated via numerical simulations in Section V.

2) VBS-MG: Since the VBS-CG algorithm is only feasible in providing a minimal GDOP value for the estimated MS within a regular polygon, the scheme may not be satisfactory for nonregular shapes of cell layout formed by the MS's neighborhood BSs. A more comprehensive scheme, i.e., the VBS-MG algorithm, is proposed in this section to further enhance

the precision of location estimation for generic cases. The main concept of the VBS-MG scheme is to iteratively select a VBS $(\boldsymbol{x}_{v,i})$ such that the newly estimated MS $(\hat{\boldsymbol{x}}^{(i-1)})$ will be located at a position with a minimal GDOP value, particularly for nonregular shapes of cell layout. The GDOP value evaluated at the $(i-1)$th estimated MS's position $(\hat{\boldsymbol{x}}^{(i-1)})$ can be formulated as

$$G_{\hat{\boldsymbol{x}}^{(i-1)}}^{(N_b+i-1)} = \left[\text{trace}(\mathbf{M}^T\mathbf{M})^{-1}\right]^{\frac{1}{2}} \tag{24}$$

where the matrix $\mathbf{M}$ is obtained as in (25). Similar to ζ_ℓ in (2) for $\ell = 1, \ldots, N_b$, $\zeta_{v,\ell} = \|\boldsymbol{x} - \boldsymbol{x}_{v,\ell}\|$ indicates the noiseless relative virtual distance for $\ell = 1, \ldots, i-1$. It is noted that the noiseless relative distances ζ_ℓ (and $\zeta_{v,\ell}$) are approximately replaced by r_ℓ (and $r_{v,\ell}$) in (25), i.e.,

$$\mathbf{M} = \begin{bmatrix} \mathbf{M}_{\text{TOA}}^{N_b \times 2} \\ \mathbf{M}_\gamma^{(i-1)\times 2} \end{bmatrix}$$

$$= \begin{bmatrix} \frac{\hat{x}^{(i-1)}-x_1}{\zeta_1} & \frac{\hat{y}^{(i-1)}-y_1}{\zeta_1} \\ \vdots & \vdots \\ \frac{\hat{x}^{(i-1)}-x_{N_b}}{\zeta_{N_b}} & \frac{\hat{y}^{(i-1)}-y_{N_b}}{\zeta_{N_b}} \\ \frac{\hat{x}^{(i-1)}-x_{v,1}}{\zeta_{v,1}} & \frac{\hat{y}^{(i-1)}-y_{v,1}}{\zeta_{v,1}} \\ \vdots & \vdots \\ \frac{\hat{x}^{(i-1)}-x_{v,i-1}}{\zeta_{v,i-1}} & \frac{\hat{y}^{(i-1)}-y_{v,i-1}}{\zeta_{v,i-1}} \end{bmatrix}$$

$$\cong \begin{bmatrix} \frac{\hat{x}^{(i-1)}-x_1}{r_1} & \frac{\hat{y}^{(i-1)}-y_1}{r_1} \\ \vdots & \vdots \\ \frac{\hat{x}^{(i-1)}-x_{N_b}}{r_{N_b}} & \frac{\hat{y}^{(i-1)}-y_{N_b}}{r_{N_b}} \\ \frac{\hat{x}^{(i-1)}-x_{v,1}}{r_{v,1}} & \frac{\hat{y}^{(i-1)}-y_{v,1}}{r_{v,1}} \\ \vdots & \vdots \\ \frac{\hat{x}^{(i-1)}-x_{v,i-1}}{r_{v,i-1}} & \frac{\hat{y}^{(i-1)}-y_{v,i-1}}{r_{v,i-1}} \end{bmatrix}$$

$$= \begin{bmatrix} \cos\theta_1 & \sin\theta_1 \\ \vdots & \vdots \\ \cos\theta_{N_b} & \sin\theta_{N_b} \\ \cos\theta_{v,1} & \sin\theta_{v,1} \\ \vdots & \vdots \\ \cos\theta_{v,i-1} & \sin\theta_{v,i-1} \end{bmatrix} \tag{25}$$

since ζ_ℓ (and $\zeta_{v,\ell}$) are considered unattainable. Moreover, the matrix $\mathbf{M}$ can further be simplified based on their corresponding angles, which implies that the GDOP value is independent of the range information r_ℓ (and $r_{v,\ell}$).

The GDOP value computed via (24) is considered under the layout of $\tilde{\mathbf{P}}_{(N_b+i-1)}(\boldsymbol{x}_1, \ldots, \boldsymbol{x}_{N_b}, \boldsymbol{x}_{v,1}, \ldots, \boldsymbol{x}_{v,i-1})$, where $\tilde{\mathbf{P}}_{(N_b+i-1)}$ denotes an arbitrary shape of the (N_b+i-1)-sided polygon. As aforementioned, the purpose of inserting the ith VBS $(\boldsymbol{x}_{v,i})$ is to make the newly estimated MS $(\hat{\boldsymbol{x}}^{(i-1)})$ possess the minimum GDOP value under the extended polygon $\tilde{\mathbf{P}}_{(N_b+i)}(\boldsymbol{x}_1, \ldots, \boldsymbol{x}_{N_b}, \boldsymbol{x}_{v,1}, \ldots, \boldsymbol{x}_{v,i})$. Therefore, the GDOP value evaluated at $\hat{\boldsymbol{x}}^{(i-1)}$ under the extended geometry $\tilde{\mathbf{P}}_{(N_b+i)}$ will become a function of the imposed VBS's position $\boldsymbol{x}_{v,i}$, i.e., $G_{\hat{\boldsymbol{x}}^{(i-1)}}^{(N_b+i)}(\boldsymbol{x}_{v,i})$. By transforming the Cartesian coordinate into the polar coordinate, the GDOP value $G_{\hat{\boldsymbol{x}}^{(i-1)}}^{(N_b+i)}(\boldsymbol{x}_{v,i})$ can be represented as $G_{\hat{\boldsymbol{x}}^{(i-1)}}^{(N_b+i)}(r_{v,i}, \theta_{v,i}) = G_{\hat{\boldsymbol{x}}^{(i-1)}}^{(N_b+i)}(\theta_{v,i})$ since $G_{\hat{\boldsymbol{x}}^{(i-1)}}^{(N_b+i)}$ is independent of $r_{v,i}$. The main purpose of the VBS-

MG scheme is to obtain the parameter $\theta_{v,i}$ such that the value of $G_{\hat{\boldsymbol{x}}^{(i-1)}}^{(N_b+i)}(\theta_{v,i})$ is minimized, i.e., to acquire the parameter $\theta_{v,i}$ such that the first-order differentiation of $G_{\hat{\boldsymbol{x}}^{(i-1)}}^{(N_b+i)}(\theta_{v,i})$ is equal to zero. After several steps of computation, the closed form of $\theta_{v,i}$ for the ith VBS $(\boldsymbol{x}_{v,i})$ can be obtained as

$$\theta_{v,i} = \arg_{\theta_{v,i}} \left\{ \frac{\partial G_{\hat{\boldsymbol{x}}^{(i-1)}}^{(N_b+i)}(\theta_{v,i})}{\partial\theta_{v,i}} = 0 \right\}$$

$$= \tan^{-1}\left(\frac{-\Gamma_2 \pm \sqrt{\Gamma_2^2 + 4\Gamma_1^2}}{2\Gamma_1}\right) \tag{26}$$

where

$$\Gamma_1 = \sum_{k=1}^{N_b} \cos\theta_k \sin\theta_k + \sum_{k=1}^{i-1} \cos\theta_{v,k} \sin\theta_{v,k} \tag{27}$$

$$\Gamma_2 = \sum_{k=1}^{N_b} \left(2\cos\theta_k^2 - 1\right) + \sum_{k=1}^{i-1} \left(2\cos\theta_{v,k}^2 - 1\right). \tag{28}$$

To acquire the position of $\boldsymbol{x}_{v,i}$, the range information $r_{v,i}$ is required to be determined in addition to the angle $\theta_{v,i}$ as in (26). Since the range $r_{v,i}$ is observed to be independent of the GDOP value from (24) and (25), the selection of $r_{v,i}$ can be determined based on the distance derived from the VBS-CG scheme at the same iteration. This type of selection for $r_{v,i}$ will be beneficial in comparing the performance of the VBS-CG and VBS-MG schemes. By adopting the same iterative process of the VBS algorithm (as shown in Fig. 4), the VBS-MG scheme will terminate its iterations until the estimation error converges to within a prespecified threshold. In the next section, the performance of the proposed VBS-CG and VBS-MG schemes will be evaluated and compared via simulations.

V. PERFORMANCE EVALUATION

Simulations are performed to show the effectiveness of the proposed VBS algorithms under different network topologies and MS's positions. The noise models and simulation parameters are illustrated in Section V-A. The performance comparison between the proposed VBS schemes with the other existing location-estimation methods is conducted in Section V-B.

A. Noise Models and Simulation Parameters

Different noise models [37] for the TOA measurements are considered in the simulations. The model for the measurement noise of the TOA signals is selected as the Gaussian distribution with zero mean and 10 m of standard deviation. Since the NLOS error is considered as a nonnegative value, an exponential distribution $p_{n_{\ell,nl}}(v)$ is assumed for the NLOS noise model of the TOA measurements, i.e.,

$$p_{n_{\ell,nl}}(v) = \begin{cases} \frac{1}{\lambda_\ell} \exp\left(-\frac{v}{\lambda_\ell}\right), & v > 0 \\ 0, & v \le 0 \end{cases} \tag{29}$$

where $\lambda_\ell = c \cdot \tau_\ell = c \cdot \tau_m \zeta_\ell^\varepsilon \rho$ for $\ell = 1$, 2, and 3. τ_ℓ is the root-mean-square delay spread between the ℓth BS and the MS;

	10%	20%	30%	40%	50%	60%	70%	80%	90%	100%
VBS-MG	24.40	33.41	48.73	67.96	83.53	98.53	116.98	140.83	197.56	467.98
VBS-CG	25.06	33.82	48.87	68.73	83.59	99.43	117.66	142.56	200.78	473.91
Two-Step LS	25.76	35.95	50.25	69.50	85.30	102.72	126.88	156.83	231.42	638.58
TSE	26.48	35.83	51.31	72.26	84.97	102.25	123.90	152.53	214.30	843.29
LLOP	25.24	34.16	49.05	70.36	84.02	101.72	127.70	156.65	216.43	502.85
RSA	25.14	34.75	49.54	70.05	84.40	100.44	126.57	154.74	215.02	497.11
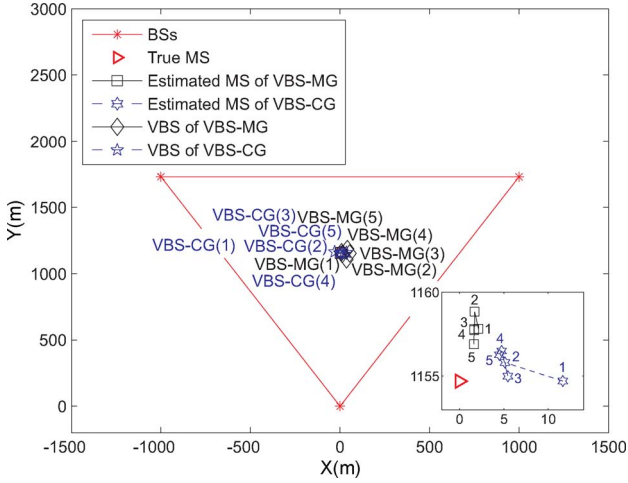
Fig. 5. Iterative processes of the VBS-MG and VBS-CG schemes for location estimation in Case 1. (Lower right subplot) Zoom-in diagram around the MS's true position (the iteration number is indicated from 1 to 5).

Fig. 6. Performance comparison of the VBS-MG and VBS-CG schemes in Case 1. Estimation errors versus numbers of VBSs.

τ_m is the median value of τ_ℓ, whose value depends on various environments, which is set as $\tau_m = 0.3$ μs. The parameter ε is the pathloss exponent, which is assumed to be 0.5, and the factor for shadow fading ρ is set to 1 in the simulations. The parameters for the noise models as previously listed in this paper primarily fulfill the environment while the MS is located within the suburban area.

The threshold parameter $\delta_{\rm th}$ (as shown in Fig. 4) for the VBS selection schemes is chosen as $\delta_{\rm th} = 0.1$ m, which indicates that the iterations will be terminated if the difference between the MS's estimated positions from two adjacent iterations is less than 0.1 m. The simulation parameters associated with four different cases are considered as follows to examine the performance of the proposed VBS algorithms. Each case is conducted with 100 runs of simulations.

Case 1) The three BSs are located at $(0, 0)$, $(1000, 1000\sqrt{3})$, and $(-1000, 1000\sqrt{3})$, which form an equilateral triangle. The MS's true position is assigned to be located at $(0, 2000\sqrt{3}/3)$, i.e., the CG of the triangle.

Case 2) The three BSs are located at $(0, 0)$, $(1000, 1000\sqrt{3})$, and $(-1000, 1000\sqrt{3})$, which form an equilateral triangle. The MS's true position is assigned to be located at $(650, 1450)$, which is comparably closer to the second BS at $(1000, 1000\sqrt{3})$.

Case 3) The three BSs are located at $(0, 0)$, $(1000, 1000\sqrt{3})$, and $(-500, 1000)$. The MS's true position is assigned to be located at $(166, 910)$, i.e., the CG of the triangle.
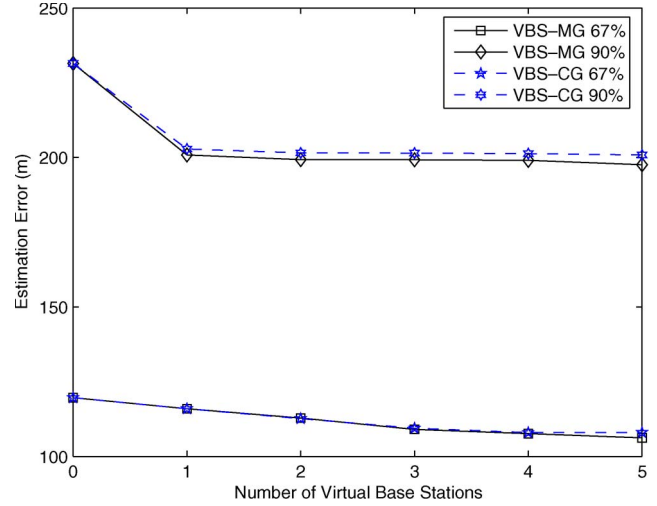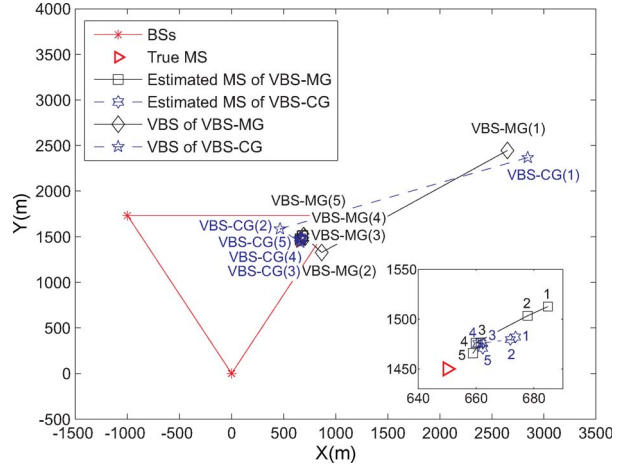

Fig. 7. Iterative processes of the VBS-MG and VBS-CG schemes for location estimation in Case 2. (Lower right subplot) Zoom-in diagram around the MS's true position (the iteration number is indicated from 1 to 5).

Case 4) The three BSs are located at $(0, 0)$, $(1000, 1000\sqrt{3})$, and $(-500, 1000)$. The MS's true position is assigned to be located at $(-250, 900)$, which is comparably closer to the third BS at $(-500, 1000)$.

B. Simulation Results

The proposed VBS algorithms (including both the VBS-CG and VBS-MG schemes) are compared with the two-step LS method [26], the TSE [5], the LLOP [7], and the RSA [10] algorithms via simulations. An equilateral triangle layout

TABLE II
PERFORMANCE COMPARISONS BETWEEN THE LOCATION-ESTIMATION SCHEMES IN CASE 2: ESTIMATION ERROR (IN METERS)

	10%	20%	30%	40%	50%	60%	70%	80%	90%	100%
VBS-MG	23.30	35.37	48.03	58.30	73.01	94.35	122.26	136.55	214.90	612.29
VBS-CG	23.31	35.47	48.23	58.32	73.63	99.34	122.76	137.14	223.22	632.59
Two-Step LS	28.21	49.68	73.81	97.69	143.02	177.24	219.69	299.76	462.75	685.35
TSE	29.19	58.34	98.05	126.67	176.15	204.56	268.22	342.18	476.49	747.31
LLOP	38.71	50.288	64.25	96.19	115.10	139.39	184.01	233.35	317.66	692.07
RSA	37.98	49.98	62.99	95.58	112.69	136.62	182.13	231.04	313.57	683.09

with the MS located at the CG of the geometry is considered in Case 1. Table I shows the performance comparison between the proposed VBS-MG and VBS-CG algorithms with other existing schemes. It is noted that the estimation error of the MS's position is represented as $\Delta \hat{x} = \|\hat{x}_f - x\|$, where $\hat{x}_f$ represents the final location estimate from the location-estimation algorithms. Since the MS is located at the CG of the equilateral triangle (i.e., with the smallest GDOP value), the performance difference between the proposed VBS algorithms and the conventional methods is not considered significant. The benefit of using the VBS schemes can be observed after 80% of position error. Due to the incorrect initial guess of the MS's position, the performance of the TSE method is comparably the worst among all the other algorithms (e.g., 843.29 m at 100% of position error). It is also noted that the nonlinear optimization (via the iterative sequential quadratic programming algorithm) involved within the RSA method requires a significant amount of computational time to obtain the estimated MS's position. In the simulations, limited iterations are conducted within the RSA scheme to preserve feasible computational efficiency.

Fig. 5 illustrates the iterative processes of the VBS-MG and VBS-CG schemes for location estimation in Case 1, which includes the following: 1) the network topology of the three BSs, i.e., the VBSs that are iteratively inserted using the VBS-MG and VBS-CG schemes, and 2) the right subplot, i.e., the zoom-in diagram around the MS's true position and the estimated MS's positions obtained from the VBS-MG and VBS-CG schemes. It is noticed that the location of each VBS is denoted as VBS-MG(ℓ) and VBS-CG(ℓ) for $\ell = 1, \ldots, 5$, where ℓ indicates the number of iterations using the VBS schemes. To decrease the GDOP value, the added VBS-MG(ℓ) is moved toward the center of the cell topology as ℓ goes from 1 to 5. On the other hand, the location of the inserted VBS-CG(ℓ) is converged to the estimated MS's position as ℓ goes to 5, which is consistent with the result obtained from Lemma 2. It is also noticed (from the zoom-in subplot of Fig. 5) that the MS's location estimates acquired from both the two VBS schemes move closer to the MS's true position as the iterations are increased.

Fig. 6 shows the estimation errors w.r.t. the number of added VBSs using the VBS-MG and VBS-CG schemes in Case 1 (with both 67% and 90% of position errors). As expected, the estimation errors are reduced as the numbers of VBSs are augmented. It can also be observed that the estimation errors quickly converge after the second VBS is inserted, which can be resulted from the ideal cell layout in Case 1, i.e., the equilateral triangle with the MS located at its CG. The ideal cell topology also keeps the performance of the VBS-MG and VBS-
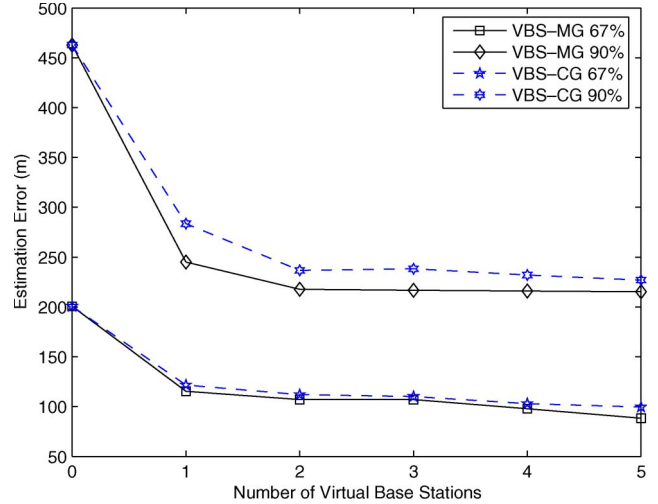

Fig. 8. Performance comparisons of the VBS-MG and VBS-CG schemes in Case 2: estimation errors versus numbers of VBSs.
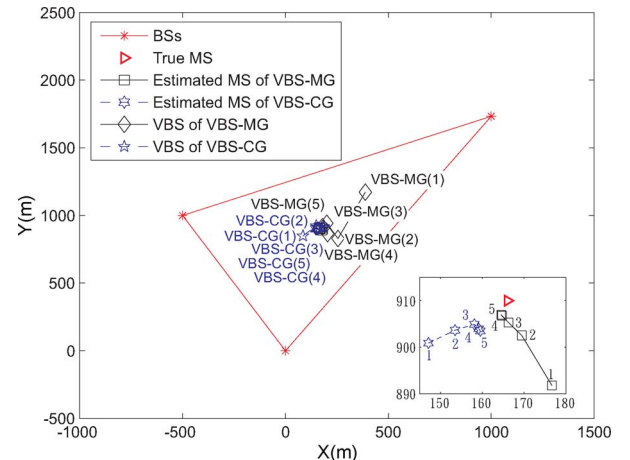

Fig. 9. Iterative processes of the VBS-MG and VBS-CG schemes for location estimation in Case 3. (Upper left subplot) Zoom-in diagram around the MS's true position (the iteration number is indicated from 1 to 5).

CG schemes similar in both 67% and 90% of position errors under the various numbers of iterations. It is also noted that the improvement on the estimated position error of the proposed VBS algorithm w.r.t. the two-step LS method can be obtained by subtracting the estimation error between VBS-MG(ℓ) and VBS-MG(0) [or between VBS-MG(ℓ) and VBS-MG(0)] for $\ell = 1, \ldots, 5$, i.e., the MS's location estimation using the two-step LS method corresponds to the cases of VBS-MG(0) and VBS-CG(0).

In Case 2, the MS's position is located closer to a BS rather than at the CG of the equilateral triangle (as shown in

TABLE III
PERFORMANCE COMPARISONS BETWEEN THE LOCATION-ESTIMATION SCHEMES IN CASE 3: ESTIMATION ERROR (IN METERS)

	10%	20%	30%	40%	50%	60%	70%	80%	90%	100%
VBS-MG	19.34	28.64	40.49	51.67	63.80	82.10	103.46	130.06	204.71	502.48
VBS-CG	19.36	28.73	41.24	51.75	67.70	83.55	107.14	145.71	209.12	532.77
Two-Step LS	21.48	39.66	45.50	54.74	71.30	88.42	118.53	163.45	258.46	945.20
TSE	20.13	33.78	44.46	50.92	72.23	86.74	109.98	147.17	270.17	951.30
LLOP	29.01	44.11	50.97	70.24	78.56	105.67	128.54	163.36	259.13	728.44
RSA	28.78	44.08	50.51	69.11	78.02	104.68	127.09	162.54	256.69	716.26

Fig. 7). Comparing with Case 1, where MS is located at the position with the smallest GDOP value, inferior performance is observed in this case by using most of the estimation schemes (as shown in Table II) due to the larger GDOP value where the MS is situated. With the assistance of VBSs, the proposed VBS algorithms consider the geometric effect on the precision of location estimation. Both of the VBS schemes can outperform the other existing schemes, as illustrated in Table II, e.g., around 100 m less of the estimation error compared with the LLOP and the RSA algorithms at 90% of position error.

It is observed in Fig. 7 that both the inserted VBS-MG(5) and VBS-CG(5) approach the estimated MS's position. The performance of both the VBS-MG and VBS-CG schemes under 67% and 90% of position errors is illustrated in Fig. 8. It is shown that a larger position error before adding any VBSs is expected [around 460 m of estimation error under 90% of position error for both VBS-MG(0) and VBS-CG(0)] due to the poor location of the MS. Performance improvement can be achieved after the first two VBSs are inserted, e.g., around 230 m of estimation error under 90% of position error for VBS-MG(2). The benefit of using the VBS-MG algorithm in comparison with the VBS-CG scheme can also be observed in Fig. 8, e.g., around 20 m less of the estimation error (under 90% of position error), by comparing VBS-MG(5) with VBS-CG(5). The reason can apparently be attributed to the fact that the VBS-CG scheme (as a simplified algorithm) was originally designed for location estimation while the MS is located closer to the CG of the cell layout with the shape of a regular polygon.

Case 3 shows the performance comparison of the location-estimation schemes under a nonequilateral triangle layout with the MS located at the CG (as shown in Fig. 9). The comparison presented in Table III shows that the VBS-MG and VBS-CG algorithms still outperform the other schemes for location estimation under this cell layout, although the MS is located at the CG of the geometry, e.g., around 15 m less of the estimation error compared with the two-step LS method (under 70% of position error). Again, the improper initial guess of the MS's position within the TSE method causes the excessive estimation error, i.e., 951.30 m at 100% of position error. As in the zoom-in subplot of Fig. 9, the improvement on the estimation errors with the augmented iterations of the VBS schemes can be acquired. The advantage of using the VBS-MG scheme compared with the VBS-CG method is still observed in this case (as shown in Fig. 10), where both schemes have converged after two iterations.

Case 4 is designed with the cell layout as a nonequilateral triangle and the MS situated closer to one of the BSs (as shown in Fig. 11), which is considered to be the most generic
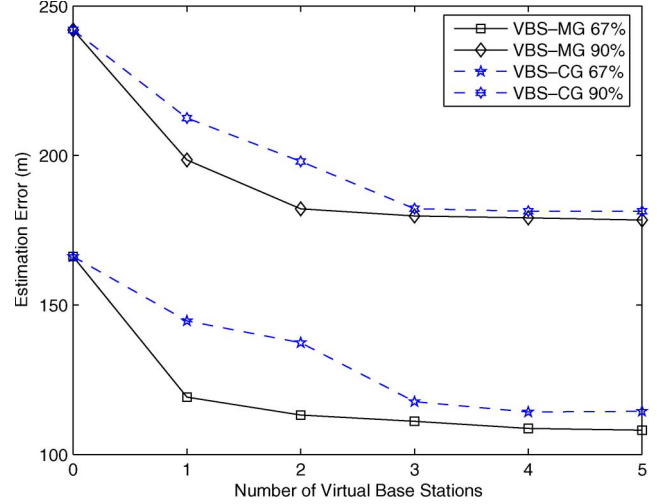

Fig. 10. Performance comparisons of the VBS-MG and VBS-CG schemes in Case 3: estimation errors versus numbers of VBSs.
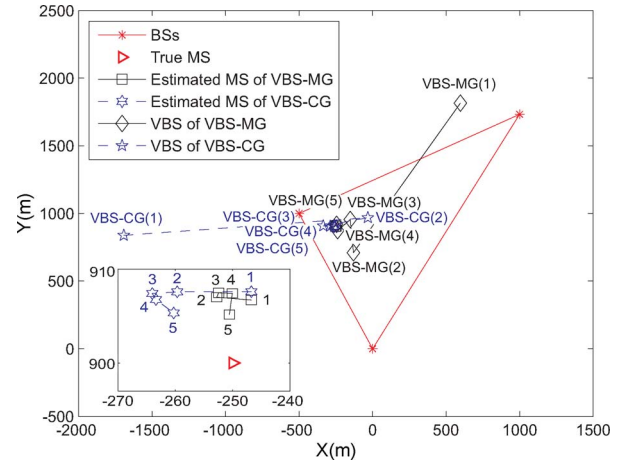

Fig. 11. Iterative processes of the VBS-MG and VBS-CG schemes for location estimation in Case 4. (Lower left subplot) Zoom-in diagram around the MS's true position (the iteration number is indicated from 1 to 5).

case. It can be seen in Table IV that the VBS-MG scheme outperforms the other algorithms under different percentages of position error, e.g., around 60 m less, by comparing the VBS-MG scheme with the RSA algorithm (under 70% of position error). To reduce the comparably higher GDOP value where the MS is located, the added VBS-MG(ℓ) are located farther away from the cell topology compared with that in Case 3. As shown in Fig. 12, around 13 m less estimation error can be acquired from VBS-MG(5) compared with VBS-CG(5) under 90% of the position error. Performance improvement can also be achieved while comparing VBS-MG(5) and VBS-MG(0),

TABLE IV
PERFORMANCE COMPARISONS BETWEEN THE LOCATION-ESTIMATION SCHEMES IN CASE 4: ESTIMATION ERROR (IN METERS)

	10%	20%	30%	40%	50%	60%	70%	80%	90%	100%
VBS-MG	18.67	27.08	43.74	53.04	61.90	80.71	104.66	130.55	192.68	359.72
VBS-CG	18.79	28.30	44.43	55.40	67.67	93.40	106.47	132.95	205.34	413.59
Two-Step LS	25.23	36.10	58.19	74.72	102.34	140.61	202.37	285.45	394.09	510.48
TSE	20.51	30.90	52.77	61.31	78.30	98.20	137.97	222.28	412.22	540.40
LLOP	30.55	47.05	58.56	70.29	94.04	134.62	168.51	222.78	299.71	502.44
RSA	29.46	45.77	56.81	68.71	91.97	131.60	166.09	218.96	295.76	497.32
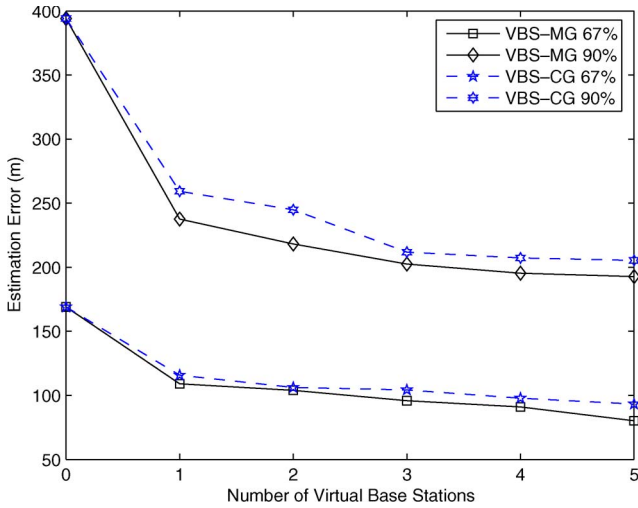
Fig. 12. Performance comparisons of the VBS-MG and VBS-CG schemes in Case 4. Estimation errors versus numbers of VBSs.
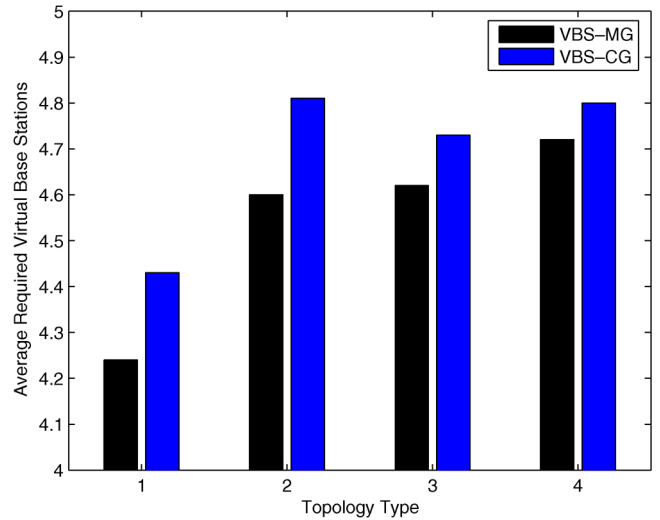

Fig. 14. Comparison between the VBS-MG and VBS-CG schemes. Average required numbers of VBSs under the four cases (with $\delta_{\text{th}} = 0.1$ m).
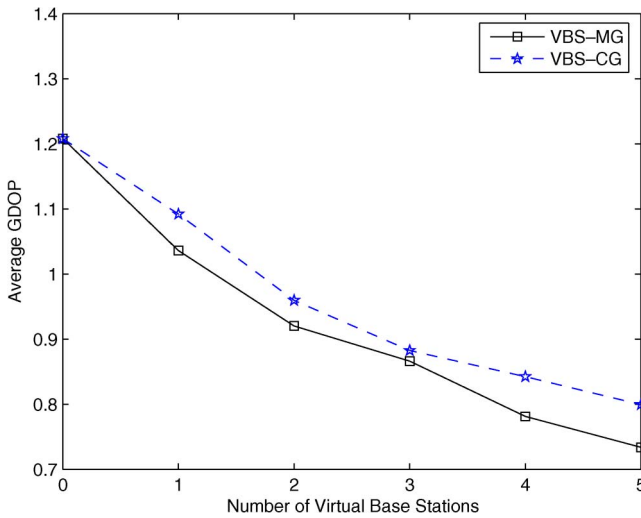

Fig. 13. Comparison between the VBS-MG and VBS-CG schemes: average GDOP values from the four cases versus numbers of VBSs.
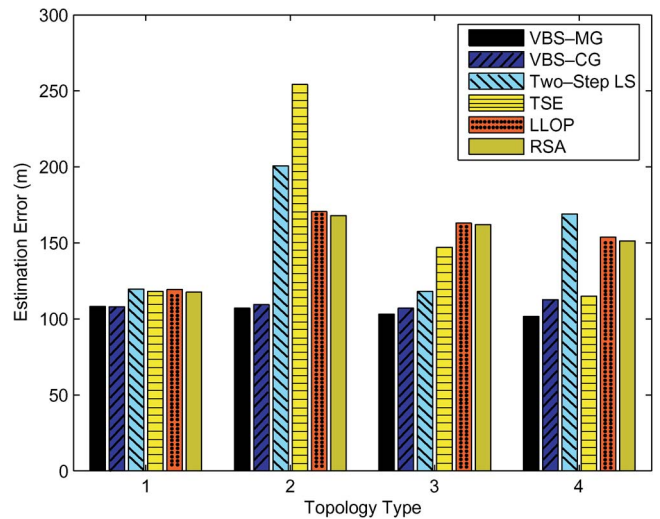

Fig. 15. Performance comparison for the location-estimation schemes under the four cases (at 67% of position error).

i.e., around 120 m less estimation error, by using the VBS-MG scheme in comparison with the two-step LS method.

Observing from the aforementioned four cases, it can be obtained that the proposed VBS-MG scheme outperforms the VBS-CG method, particularly while the MS is not located at a position with a minimal GDOP value. Fig. 13 illustrates the comparison between the VBS-MG and VBS-CG schemes by considering the average GDOP values obtained from the aforementioned four cases under different numbers of VBSs.

It can be observed that the VBS-MG scheme can acquire a lower average GDOP value in each iteration than that obtained from the VBS-CG method. The reason can obviously be attributed to the inherent design to have the minimal GDOP value within the VBS-MG formulation. Moreover, the average required number of VBSs within the four cases is shown in Fig. 14 with the iteration threshold $\delta_{\text{th}} = 0.1$ m. On average, the VBS-CG scheme requires more VBSs compared with the VBS-MG method to achieve the same iteration threshold value,

i.e., around 4.83 VBSs on average are required for VBS-CG, whereas only 4.62 VBSs are required for VBS-MG in Case 2. However, both VBS schemes are able to reach a similar level of estimation errors after the insertion of two to three VBSs, as observed in Figs. 6, 8, 10, and 12. These two proposed VBS algorithms can be converged within two to three iterations to achieve feasible precision for location estimation. Fig. 15 illustrates the overall performance comparison between the location-estimation schemes under the four different cases at 67% of position error. The proposed VBS algorithms can effectively promote the precision for location estimation under various geometric topologies that are associated with the NLOS noises.

VI. Conclusion

Location-estimation algorithms with the assistance of VBSs have been proposed in this paper. The proposed VBS schemes enhanced the conventional two-step LS algorithm by imposing additional information from the VBSs within its formulation. By using the proposed VBS algorithms, the computational efficiency acquired from the two-step LS method was preserved. Moreover, higher location-estimation accuracy for the MS was also achieved, particularly under the NLOS environments. The two proposed schemes, namely, VBS-CG and VBS-MG, iteratively select the VBSs by considering the GDOP value associated with the geometric relationship between the MS and the cell layout. It has been shown in the simulation results that the proposed VBS-MG scheme provides better accuracy for location estimation compared with other existing network-based positioning methods.

References

[1] Fed. Commun. Comm. (FCC), "Revision of the commission's rules to ensure compatibility with enhanced 911 emergency calling systems," U.S. FCC, Washington, DC, FCC Rep. CC Docket No. 94-102, RM-8143, Jun. 1996.

[2] Y. Zhao, "Standardization of mobile phone positioning for 3G systems," *IEEE Commun. Mag.*, vol. 40, no. 7, pp. 108–116, Jul. 2002.

[3] H. Koshima and J. Hoshen, "Personal locator services emerge," *IEEE Spectr.*, vol. 37, no. 2, pp. 41–48, Feb. 2000.

[4] J. H. Reed, K. J. Krizman, B. D. Woerner, and T. S. Rappaport, "An overview of the challenges and progress in meeting the E-911 requirement for location service," *IEEE Commun. Mag.*, vol. 36, no. 4, pp. 30–37, Apr. 1998.

[5] W. H. Foy, "Position-location solutions by Taylor-series estimation," *IEEE Trans. Aerosp. Electron. Syst.*, vol. AES-12, no. 2, pp. 187–194, Mar. 1976.

[6] Y. T. Chan and K. C. Ho, "A simple and efficient estimator for hyperbolic location," *IEEE Trans. Signal Process.*, vol. 42, no. 8, pp. 1905–1915, Aug. 1994.

[7] J. J. Caffery, "A new approach to the geometry of TOA location," in *Proc. IEEE VTC*, Boston, MA, Sep. 2000, vol. 4, pp. 1943–1949.

[8] J. J. Caffery and G. L. Stüber, "Subscriber location in CDMA cellular networks," *IEEE Trans. Veh. Technol.*, vol. 47, no. 2, pp. 406–416, May 1998.

[9] S. S. Woo, H.-R. You, and J. S. Koh, "The NLOS mitigation technique for position location using IS-95 CDMA networks," in *Proc. IEEE VTC*, Boston, MA, Sep. 2000, vol. 6, pp. 2556–2560.

[10] S. Venkatraman, J. J. Caffery, and H. R. You, "A novel TOA location algorithm using LOS range estimation for NLOS environments," *IEEE Trans. Veh. Technol.*, vol. 53, no. 5, pp. 1515–1524, Sep. 2004.

[11] N. Levanon, "Lowest GDOP in 2-D scenarios," *Proc. Inst. Elect. Eng.—Radar Sonar Navig.*, vol. 147, no. 3, pp. 149–155, Jun. 2000.

[12] R. O. Schmidt, "Multiple emitter location and signal parameter estimation," *IEEE Trans. Antennas Propag.*, vol. AP-34, no. 3, pp. 276–280, Mar. 1986.

[13] E. G. Strom, S. Parkvall, S. L. Miller, and B. E. Ottersten, "Propagation delay estimation of DS-CDMA signals in a fading environment," in *Proc. IEEE GLOBECOM*, San Francisco, CA, Nov. 1994, pp. 85–89.

[14] B. M. Radich and K. M. Buckley, "The effect of source number underestimation on MUSIC location estimates," *IEEE Trans. Signal Process.*, vol. 42, no. 1, pp. 233–236, Jan. 1994.

[15] P. Luukkanen and J. Joutsensalo, "Comparison of MUSIC and matched filter delay estimators in DS-CDMA," in *Proc. IEEE PIMRC*, Helsinki, Finland, Sep. 1997, vol. 3, pp. 830–834.

[16] S. Gazor, S. Affes, and Y. Grenier, "Robust adaptive beamforming via target tracking," *IEEE Trans. Signal Process.*, vol. 44, no. 6, pp. 1589–1593, Jun. 1996.

[17] S. Affes, S. Gazor, and Y. Grenier, "An algorithm for multisource beamforming and multitarget tracking," *IEEE Trans. Signal Process.*, vol. 44, no. 6, pp. 1512–1522, Jun. 1996.

[18] K. Harmanci, J. Tabrikian, and J. L. Krolik, "Relationships between adaptive minimum variance beamforming and optimal source localization," *IEEE Trans. Signal Process.*, vol. 48, no. 1, pp. 1–12, Jan. 2000.

[19] K. Kaemarungsi and P. Krishnamurthy, "Properties of indoor received signal strength for WLAN location fingerprinting," in *Proc. IEEE MOBIQUITOUS*, Boston, MA, Aug. 2004, pp. 14–23.

[20] J. Kwon, B. Dundar, and P. Varaiya, "Hybrid algorithm for indoor positioning using wireless LAN," in *Proc. IEEE VTC*, Los Angeles, CA, Sep. 2004, vol. 7, pp. 4625–4629.

[21] K. Kaemarungsi and P. Krishnamurthy, "Modeling of indoor positioning systems based on location fingerprinting," in *Proc. IEEE INFOCOM*, Hong Kong, Mar. 2004, vol. 2, pp. 1012–1022.

[22] S. Y. Tan and H. S. Tan, "Improved three-dimensional ray tracing technique for microcellular propagation models," *Electron. Lett.*, vol. 31, no. 17, pp. 1503–1505, Aug. 1995.

[23] Z. Sandor, L. Nagy, Z. Szabo, and T. Csaba, "3D ray launching and moment method for indoor radio propagation purposes," in *Proc. IEEE PIMRC*, Oulu, Finland, Sep. 1997, vol. 1, pp. 130–134.

[24] M. Hata, "Empirical formula for propagation loss in land mobile radio services," *IEEE Trans. Veh. Technol.*, vol. VT-29, no. 3, pp. 317–325, Aug. 1980.

[25] S. Y. Seidal and T. S. Rappaport, "Site-specific propagation prediction for wireless in-building personal communication system design," *IEEE Trans. Veh. Technol.*, vol. 43, pp. 879–891, Nov. 1994.

[26] X. Wang, Z. Wang, and B. O'Dea, "A TOA-based location algorithm reducing the errors due to non-line-of-sight (NLOS) propagation," *IEEE Trans. Veh. Technol.*, vol. 52, no. 1, pp. 112–116, Jan. 2003.

[27] L. Cong and W. Zhuang, "Hybrid TDOA/AOA mobile user location for wideband CDMA cellular systems," *IEEE Trans. Wireless Commun.*, vol. 1, no. 3, pp. 439–447, Jul. 2002.

[28] S. Venkatraman and J. J. Caffery, "Hybrid TOA/AOA techniques for mobile location in non-line-of-sight environments," in *Proc. IEEE WCNC*, Atlanta, GA, Mar. 2004, vol. 1, pp. 274–278.

[29] P. C. Chen, "A non-line-of-sight error mitigation algorithm in location estimation," in *Proc. IEEE WCNC*, New Orleans, LA, Sep. 1999, vol. 1, pp. 316–320.

[30] M. P. Wylie and J. Holtzman, "The non-line of sight problem in mobile location estimation," in *Proc. IEEE ICUPC*, Cambridge, MA, Sep. 1996, vol. 2, pp. 827–831.

[31] J. Borras, P. Hatrack, and N. B. Mandayam, "Decision theoretic framework for NLOS identification," in *Proc. IEEE VTC*, Ottawa, ON, Canada, May 1998, vol. 2, pp. 1583–1587.

[32] B. L. Le, K. Ahmed, and H. Tsuji, "Mobile location estimator with NLOS mitigation using Kalman filtering," in *Proc. IEEE WCNC*, New Orleans, LA, Mar. 2003, vol. 3, pp. 1969–1973.

[33] K. T. Feng, C. L. Chen, and C. H. Chen, "GALE: An enhanced geometry-assisted location estimation algorithm for NLOS environments," *IEEE Trans. Mobile Comput.*, vol. 7, no. 2, pp. 199–213, Feb. 2008.

[34] C. L. Chen and K. T. Feng, "An efficient geometry constrained location estimation algorithm for NLOS environments," in *Proc. IEEE Int. Conf. WirelessCom*, Maui, HI, Jun. 2005, pp. 244–249.

[35] C. L. Chen and K. T. Feng, "Enhanced location estimation with the virtual base stations in wireless location systems," in *Proc. IEEE VTC*, Melbourne, Australia, May 2006, pp. 603–607.

[36] J. Chaffee and J. Abel, "GDOP and the Cramer–Rao bound," in *Proc. IEEE PLANS*, Las Vegas, NV, Apr. 1994, pp. 663–668.

[37] L. J. Greenstein, V. Erceg, Y. S. Yeh, and M. V. Clark, "A new path-gain/delay-spread propagation model for digital cellular channels," *IEEE Trans. Veh. Technol.*, vol. 46, no. 2, pp. 477–485, May 1997.

Chien-Hua Chen (S'07) received the B.S. degree in electrical engineering from the National Cheng Kung University, Tainan, Taiwan, in 2002 and the M.S. degree in communication engineering from the National Chiao Tung University, Hsinchu, Taiwan, in 2006. He is currently working toward the Ph.D. degree with the Department of Communication Engineering, National Chiao Tung University.

His current research interests include wireless location technologies and MAC layer issues for Wi-Fi systems.

Kai-Ten Feng (M'03) was born in Taipei, Taiwan, in 1970. He received the B.S. degree from the National Taiwan University, Taipei, in 1992, the M.S. degree from the University of Michigan, Ann Arbor, in 1996, and the Ph.D. degree from the University of California, Berkeley, in 2000.

Between 2000 and 2003, he was an In-Vehicle Development Manager/Senior Technologist with OnStar Corporation USA, which is a subsidiary of General Motors Corporation. His major responsibilities with OnStar included the design of future telematics platforms and in-vehicle networks. Between February 2003 and July 2007, he was an Assistant Professor with the Department of Communication Engineering, National Chiao Tung University, Hsinchu, Taiwan, where he has been an Associate Professor since August 2007. His current research interests include cooperative and cognitive networks, mobile ad hoc and sensor networks, embedded system design, wireless location technologies, and intelligent transportation systems.

Dr. Feng has served on the Technical Program Committees of the IEEE Vehicular Technology Conference, the IEEE International Conference on Communications, and the IEEE Asia Pacific Wireless Communications Symposium. He was the recipient of the Best Paper Award at the Spring 2006 IEEE Vehicular Technology Conference and the Outstanding Young Electrical Engineer Award from the Chinese Institute of Electrical Engineering in 2007.

Chao-Lin Chen received the B.S. and M.S. degrees in communication engineering from the National Chiao Tung University, Hsinchu, Taiwan, in 2003 and 2006, respectively.

He was with the Department of Electronics Engineering, National Chiao Tung University, as a Teaching Assistant between August 2006 and July 2007. Since October 2007, he has been with TrendChip Technologies Corporation, Hsinchu, as an Executive Engineer. His current research interests include wireless location technologies, cooperative networks, and cognitive networks.
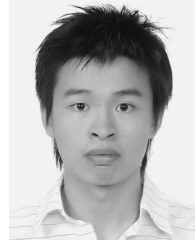
Po-Hsuan Tseng (S'08) received the B.S. degree in communication engineering in 2005 from the National Chiao Tung University, Hsinchu, Taiwan, where he is currently working toward the Ph.D. degree with the Department of Communication Engineering.

His current research interests include wireless location technologies and mobile WiMax system design.